

Investigation of Selected Silicon Nitride and Silicon Carbide Ceramics

N. L. HECHT, D. E. McCULLUM, AND G. A. GRAVES

University of Dayton
Dayton, Ohio

A project at the University of Dayton Research Institute investigating the Environmental Effects in Toughened Ceramics was extended to investigate SiC and Si₃N₄ ceramics which are candidates for heat engine applications. Three materials (two Si₃N₄ and one SiC) were selected for characterization and evaluation. Microstructure, chemistry, physical, and mechanical properties at 25° and 1450°C were investigated.

Introduction

As part of this investigation a literature review was conducted which concentrated on the proceedings and agendas for technical meetings concerned with the development of ceramics for heat engine applications. The investigation and development of SiC and Si₃N₄ materials for heat engine applications dates back to the late 1960s, and in the ensuing years a significant body of literature concerning these materials has accumulated. Major emphasis has been placed on monolithic silicon nitride (Si₃N₄) and silicon carbide (SiC) ceramics. More recently, attention has focused to some extent on SiC and Si₃N₄ composites. From the literature review it became apparent that a large number of SiC and Si₃N₄ ceramics have been studied. A significant portion of the literature describes characterization studies performed and the property values obtained. However, these studies were not always systematically conducted, the test methods were not always well documented, and the reporting procedures varied. As a result, the property data available in the literature are somewhat incomplete and inconsistent.

The properties and behavior of the SiC and Si₃N₄ ceramics have been measured and studied by a variety of test methods and in a number of different environments. Microstructure, density, elastic modulus, coefficient of thermal expansion, thermal conductivity, flexure strength, fracture toughness, creep, stress rupture, and oxidation behavior were the properties most frequently reported. Physical and mechanical properties at room temperature have been measured for almost all of the materials described in the literature. Properties have also been measured for some of these materials to temperatures in excess of 1400°C.

Property data available for the various SiC and Si₃N₄ ceramics were compiled and consolidated according to fabrication category. This compilation is presented in Table I which provides both the mean and range of values reported for each material category. Flexure strength, tensile strength, and elastic modulus property values are reported at both room temperature and 1400°C. It should be noted that several materials failed at temperatures below 1400°C. The creep data compiled are for steady state conditions (type II creep) and follow the relationship

$$\dot{\epsilon} = A^n e^{-Q/RT} \quad (1)$$

parameter, S_0 (the 63rd percentile for the distribution of breaking strength) were determined. Upper and lower bounds at the 90% confidence limits were also calculated.

The elastic modulus of three representative specimens of each candidate material was measured by a Grindo-Sonic (Model MR3ST) Transient Impulse/Elastic Modulus Apparatus. Hardness was measured on five representative samples from each candidate material using a Vickers microindent hardness tester.

The microstructure and chemistry of the three candidate materials were also studied. Polished sections from representative specimens were viewed by optical microscope (Nikon Epiphot) and freshly fractured sections were viewed by scanning electron microscope (JOEL JSM-840). X-ray fluorescence (EDXA) spectra were obtained using the EG&G Ortec System 5000 attached to the JSM-840. Test specimens were also examined by X-ray diffraction (GE-XRD6).

Fracture toughness was measured for the three materials by two different techniques: the controlled flaw method and the microindent method. Fracture toughness (K_{Ic}) by the controlled surface flaw method is determined from the relationship

$$K_{Ic} = 2.06 \sigma_f \sqrt{c/\pi} \quad (2)$$

where σ_f = flexure strength measured by 3-point bend test, and c = the radial crack extension of the microindent. K_{Ic} by the microindentation technique can be estimated from the data obtained using one of the following two equations:

$$K_{Ic} = (\hat{c}/\hat{a})^{-3/2} (H/E\theta)^{2/5} (H \sqrt{A}/\theta) \quad (3)$$

or

$$K_{Ic} = 0.15 k (\hat{c}/\hat{a})^{-3/2} (H \sqrt{a}/\theta) \quad (4)$$

where $\theta \approx 3$ (constraint factor), $k \approx 3.2$ (correction for free surface), H is the measured hardness, \hat{a} is one-half the indent diagonal, \hat{c} is the radial crack extension, and E is the elastic modulus.

Results and Discussion

The density, elastic modulus, and hardness values measured for the three candidate materials are presented in Table IV. The density measurements indicate that all three materials are approximately 99% of the calculated theoretical density. The average density, elastic modulus, and hardness values measured were within the published range of values reported for these materials; however, the hardness values measured were slightly lower than the average values reported.

SEM photomicrographs of the flexure tested material at 25° and 1450°C are presented in Figs. 2 through 7. The results of the X-ray diffraction analysis spectra obtained from the candidate materials after flexure testing at 25° and 1450°C are presented in Tables V to VII.

The results of the flexure strength measurements for the three materials at 25° and 1450°C are presented in Table VIII. The results of the Weibull analysis for the flexure test data are presented in Table IX.

The room temperature flexure strength values obtained for α -SiC were in good agreement with the published values. However, the strength values measured for the PY6 material were about 10% higher than published values and the strength values for the XL144 material were about 30% lower than manufacturer's pub-

lished values. The flexure strengths measured for all three materials at 1450°C are more than 30% higher than the average strength values published for these materials. The two Si₃N₄ materials tested at 1450°C were observed to have undergone considerable oxidation when examined after testing. The α-SiC specimens did not appear to have undergone any observable oxidation. It is estimated that during flexure strength testing at 1450°C the test specimens are above 1000°C for about four hours. From the XRD analysis it was found that both cristobalite and Y₂Si₂O₇ formed on the surface of the Si₃N₄ test specimens.

Fracture origins were determined using optical microscope and SEM techniques. Examination of the fractured test bars showed that at room temperature all of the Hexoloy specimens failed due to tensile surface flaws. The PY6 and XL144 materials failed at both tensile surface and edge flaws. At 1450°C it was observed that the Hexoloy specimens failed at tensile surface and edge flaws and the PY6 material failed at tensile surface, edge, and subsurface flaws. The XL144 material tested at 1450°C failed primarily due to tensile surface flaws; however, two of the test specimens failed at edge flaws and one specimen failed at a subsurface inclusion. It was further observed that failure initiation for the PY6 material at elevated temperature was frequently at a surface or subsurface inclusion (see Figs. 8 and 9). The inclusion failure site shown in Fig. 9 was examined by EDXA and found to contain Fe, Cr, and Cu contaminants.

Similar inclusions were also observed on the surface of untested PY6 specimens. A typical inclusion is shown in Fig. 10. This inclusion was also examined by EDXA and found to contain Mo. The presence of Mo and Fe inclusions in sintered Si₃N₄ materials has been reported by Helms, et al.,¹ Larsen,² and Pasto.³ Similar metal inclusions were also observed in the Norton Noralide XL144 material.

The results of the fracture toughness (K_{Ic}) measurements are presented in Table X. Typical indents are shown in Figs. 11 through 13. For the PY6 and XL144 materials an indent load of 2.6 kg was used. However, for the α-SiC material a load of 500 grams was used. The higher indent load crushed the α-SiC specimens and the lower load had to be used to obtain acceptable indents. The fracture toughness values measured by the microindent technique tended to be higher than the toughness values measured by the controlled flaw method. However, almost all the values measured were lower than published or reported by the manufacturer.

The results of the thermal expansion measurements are presented in Table XI. The coefficient of thermal expansion measured for both Si₃N₄ materials were in close agreement with published values for these materials. However, the average coefficient measured for α-SiC was more than 17% higher than reported for this material. The standard deviation calculated for the SiC material was relatively small (about 7-1/2%); however, the standard deviation calculated for the two Si₃N₄ materials were significantly higher (about 16%). In addition, the retesting of the Si₃N₄ specimens resulted in substantial differences in measured coefficient of expansion. This difference may be due to oxidation of the test specimen during the initial test cycle. The coefficient of thermal expansion tended to decrease when measured during the second test cycle for the Si₃N₄ material. Based on limited data it would appear that the measured coefficient stabilizes after the first test cycle.

Conclusions

This project provided a limited evaluation for three candidate SiC/Si₃N₄ materials. From the results obtained it can be concluded:

1. In general, the property values measured were in agreement with published values for these materials.
2. The data obtained in this limited study indicate that the Hexoloy α -SiC material offers greater promise for structural application at temperatures of 1450°C than the other two materials studied.
3. This project also provided important insights into the procedures for effective property evaluation of the SiC and Si₃N₄ ceramics.
 - a. It is desirable to use more test specimens (25) per test temperature for strength measurements. It is also desirable to measure strength at three or four different temperatures.
 - b. Tensile and fatigue property data are also very important to obtain in the characterization of candidate ceramic materials for heat engine applications. These data are critical to the selection and design of engine components.
 - c. To obtain consistent values for the coefficient of thermal expansion it is desirable to measure each test specimen at least three times.
 - d. Chemical analysis and identification of inclusions are imperative.
 - e. Since the potential application for these materials is for use at extended times in oxidizing environments at high temperature (1400°C), it is important to measure the mechanical strength under these conditions. The mechanical strength of candidate materials should be monitored at elevated temperature (1400°C) after significant exposure (hundreds of hours) under nominal loading.

Acknowledgments

This work was funded by the Department of Energy through a subcontract with Martin Marietta Energy Systems, Inc. at Oak Ridge National Laboratory. The authors wish to acknowledge the support and assistance of Dr. V. J. Tennery, Contract Monitor. We would also like to thank Dr. P. Yaney of the Department of Physics for the Raman studies. In addition we would like to acknowledge the work of Mr. J. D. Wolf for the SEM and X-ray diffraction analyses, and Dr. A. Berens for the statistical analysis. The important contributions of Stephen Goodrich, Dale Grant, and Stan Hilton are also acknowledged.

References

- ¹Helms, H. E., P. W. Heitman, L. C. Lindgren, and S. R. Thrasher, *Ceramic Applications in Turbine Engines*, Noyes Publications, New Jersey, 1986.
- ²Larsen, D. C. and J. W. Adams. "Property Screening and Evaluation of Ceramic Turbine Materials," ADA 142739, April 1984.
- ³Pasto, A. E., J. T. Neil, and C. L. Quackenbush, "Microstructural Effects Influencing Strength of Sintered Silicon Nitride," in *Proc. of International Conf. on Ultrastructure Processing of Ceramics, Glasses, and Composites*, 1984.

Table I. Summary of Reported Property Values for Si₃N₄ and SiC

Material Type	Young's Modulus (GPa)		Fracture Toughness (MPa·√m)	Creep Activation Energy (kcal/mol)	Density (g/cm ³)	CTE 20°-1000°C (10 ⁻⁶ /°C)	Oxidation Weight Gain (%/1000 h)		Flexure Strength (MPa)		Tensile Strength (MPa)	
	20°C	1400°C					20°C	1400°C	20°C	1400°C	20°C	1400°C
Hot-pressed Si ₃ N ₄ (range)	300	175	4.8*	110	3.18	3.3	0.75	750	300†	375	150	
	250-325	175-250	2.8-6.6	0.05-2.5	3.07-3.37	3-3.9	0.05-2.5	450-1100	0-600			
Sintered Si ₃ N ₄ (range)	245	195-315	4.3	114	3.13	3.5	0.2	415	70			
			3-5.6		2.8-3.4			275-840	0-700			
Reaction-sintered Si ₃ N ₄ (range)	175	155	3.6	82	2.4	2.9	1.5	200	250	170	140	
	100-220	120-200			2.0-2.8	2.5-3.1	0.10-2.6	50-300	0-400	70-210		
Hot-pressed SiC (range)	440	380	3.9	0.9	3.23	4.55	0.3	500	300	200	35-150	
	430-450		3-4		3.2-3.3	4.3-5.4	0.1-0.6	300-800	175-575			
Sintered SiC (range)	395	372	4	230	3.1	4.5	0.1	375	380			
	375-420	300-400	2.5-6.5		3.0-3.2	4.4-4.8	0.01-0.25	275-535	240-450			
Reaction-sintered SiC (range)	360	275		235	3.0	4.33	0.1	310	190	77		
	350-375	200-320			2.9-3.1	4.3-4.4	0.06-0.16	175-450	70-450			

*K_{IC} increases above 1000°C.

† Above 1200°C, dynamic fatigue shows slow crack growth.

Table II. Reported Characterization Information for Candidate Materials

Material	Fabrication Method	Chemistry	MOR _{RT} * (MPa)	MOR ₄₀₀ (MPa)	Elastic Modulus (GPa)	Fracture Toughness (MPa·√m)	Hardness (kg/mm ²)	Coefficient Thermal Expansion (10 ⁻⁶ /°C(20°-1000°))	Grain Size (μm)
GTE-PY6	Injection-molded and hiped	β-Si ₃ N ₄ + 6 wt% Y ₂ O ₃ Trace-Al, Fe, Mo	550-950 (800)	70-275	245-290	4-4.5		3.5	0.5-3
Sohio Hexology	Pressureless-sintered (formed by pressing or injection or isostatic forming)	α-SiC + 0.5 β Trace Al, Fe, Ti	300-350	370-380	300	4	2740	4.5	2-8
Norton XL 144	Hot-pressed	β-Si ₃ N ₄ -no other data	770	300-350	370-395	4-4.5	1600	3.5	3-5

*MOR = Flexure strength.

Table III. Characterization Protocol

Measurement	Technique/Conditions	Number of Specimens
Microstructure	SEM/optical microscope	3
Chemistry	XRD/EDXA, Auger	3
Density	Immersion at 25°C	5
Hardness	Microhardness at 25°C	5
Thermal expansion*	Temp. Range 25°–1450°C	4
Fracture toughness [†]	Microindent and controlled flaw at 25°C	10
Flexure strength [‡]	At 25°C and 1450°C	10/10
Elastic modulus	Sonic velocity	3

*Thermal expansion was measured on four specimens no less than two times for at least three of the specimens from 25° to 1450°C using a Theta Industries Dilatronic II (Model 6024) to determine if expansion hysteresis effects are present.

[†]Fracture toughness was measured by microindentation and controlled flaw techniques; a comparison of the toughness values will be made.

[‡]Flexure strength was measured in four-point flexure with an outer span of 3.81 cm (1.50 in.), an inner span of 1.91 cm (0.75 in.), and a specimen cross section of 0.64 × 0.32 cm (0.250 × 0.125 in.), with specimens loaded at a rate of 0.051 cm/min (0.020 in./min); 10 specimens were used at each test condition.

Table IV. Room-Temperature Physical Property Values Measured for the SiC and Si₃N₄ Ceramics

Material	Density (g/cm ³)	Modulus (GPa)	Hardness (Std. Dev.) (GPa)
GTE-PY6	3.24	293	1458 (118)
Noralide XL144	3.23	314	1421 (52)
Hexoloy α-SiC	3.17	427	2588 (80)

Table V. X-Ray Diffraction Analysis for GTE-PY6

2 θ	Intensity ($I/I_{max} = 100$)	Crystal Phase	
		As-Received	After 1450°C
21.95	92		C [§]
23.4	29/27	β^*	β
26.5	6/1	? α^\dagger	? α
27.1	82/94	β	β
27.75	6		Y
28.4	4		C
29.5	3		Y
29.7	6	?Y [‡]	
31.45	11		C
33.7	85		β
33.9	88	β	
36.1	100	β	β
37.1	6		
37.6	6		
39.0	12/11	β /Y	β /Y
41.5	29/36	β	β
48.0	12	β	
50.0	18	β	
52.2	41	β	
58.0	18	β	

* β = β -phase Si_3N_4 .[†] α = α -phase Si_3N_4 .[‡]Y = $\text{Y}_2\text{Si}_2\text{O}_7$.[§]C = cristobalite.

Table VI. X-Ray Diffraction Analysis for Norton Noralide XL144

2 θ	Intensity ($I/I_{max} = 100$)	Crystal Phase	
		As-Received	Tested at 1450°C
21.95	24		C*
23.4	25		β^{\dagger}
23.55	29	β	
27.1	97		β
27.25	97	β	
27.7	6		Y^{\ddagger}
29.45	8		Y
31.45	1		C
32.75	1		
33.25	5		
33.7	33		β
33.85	39	β	
36.1	100		β
36.25	100	β	
39.0	4		
39.2	6	β	
39.7	1		Y
41.45	13		β
41.6	13	β	
48.05	11	β	
50.1	12	β	
52.4	24	β	

*C = cristobalite.

 $\dagger\beta$ = β -phase Si_3N_4 . $\ddagger Y$ = $Y_2Si_2O_7$.

Table VII. X-Ray Diffraction Analysis for Sohio Hexoloy- α -SiC

2 θ	Intensity ($I/I_{max} = 100$)	Crystal Phase	
		As-Received	Tested at 1450°C
22.0	9		C*
24.9	3		
26.75	1		
34.2	25/33	α^\dagger	α
34.95	4/8		α
35.75	100	α	α
38.25	31/36	α	α
41.5	13/17	α	α
45.4	6/8	α	α
55.0	7	α	
60.0	60	α	

*C = cristobalite.

† = α -phase SiC.

Table VIII. Measured Flexure Strength at 25° and 1450°C

Material	Temperature (°C)	Average Strength (MPa)	Std. Deviation (MPa)	95% Confidence Limit (MPa)
GTE-PY6	25	641	69	592–691
GTE-PY6	1450	393	69	343–442
Norton XL144	25	538	97	467–607
Norton XL144	1450	453	53	415–491
Sohio α -SiC	25	331	41	302–360
Sohio α -SiC	1450	500	52	463–538

Table IX. Summary of Weibull Analysis Results

Material Designation	Test Temp. (°C)	Average Strength (MPa)	Shape Parameter (M)	Shape Parameter (S ₀)	Confidence Bounds			
					M	S ₀	LCL*	UCL [†]
GTE-PY6	25	641	10.80	671	LCL*	UCL [†]	LCL	UCL
GTE-PY6	1450	393	8.30	419	5.94	14.69	632	714
Hexology SiC	25	331	8.90	349	4.57	11.25	388	454
Hexology SiC	1450	500	9.88	524	4.90	12.10	342	376
Norton XL144	25	538	6.06	578	5.43	13.44	490	560
Norton XL144	1450	453	12.02	474	3.33	8.24	520	645
					6.61	16.35	449	501

*LCL = lower confidence limit.

†UCL = upper confidence limit.

Table X. Fracture Toughness (K_{Ic}) Measurements

Material	Ave. K_{Ic} by Microindent (MPa · \sqrt{m})	Ave. K_{Ic} by Controlled Flaw (MPa · \sqrt{m})
GTE-PY6	6.1	3.0
Norton XL144	3.8	3.1
Sohio α -SiC	2.6	2.1

Table XI. Thermal Expansion Test Results

Material	Specimen Number	Temp. (°C)	CTE ($\times 10^{-6}$)
Noralide XL144	A	1460	3.3
	B	1200	4.0
Norton Si ₃ N ₄		1250	3.6
	C	1465	2.9
		1475	3.3
	D	1450	4.2
		1450	2.7
		Average	3.4
		Std. Dev.	0.5
PY6	A	1450	4.2
		1480	3.0
GTE Si ₃ N ₄	B	1425	4.3
		1450	2.8
		1450	2.9
	C	1390	4.0
		1475	3.0
	D	1460	3.3
		Average	3.4
		Std. Dev.	0.6
Hexoloy SA	A	1460	5.2
		1460	5.1
Sohio SiC	B	1465	5.9
		1475	5.2
	C	1465	5.8
		1475	5.0
	D	1410	5.7
		Average	5.4
	Std. Dev.	0.4	

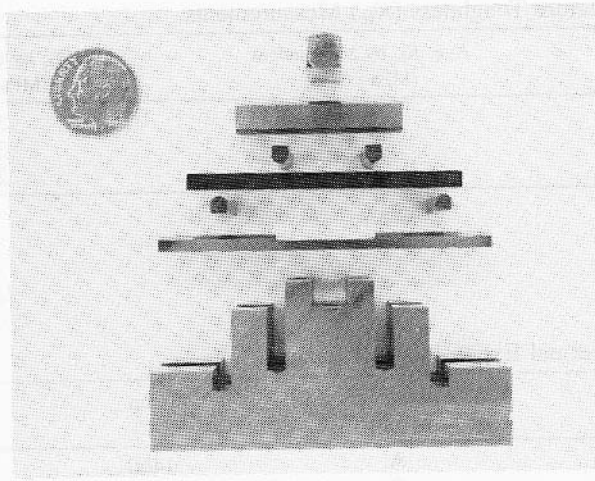


Fig. 1. The four-point bend fixture for flexure testing.

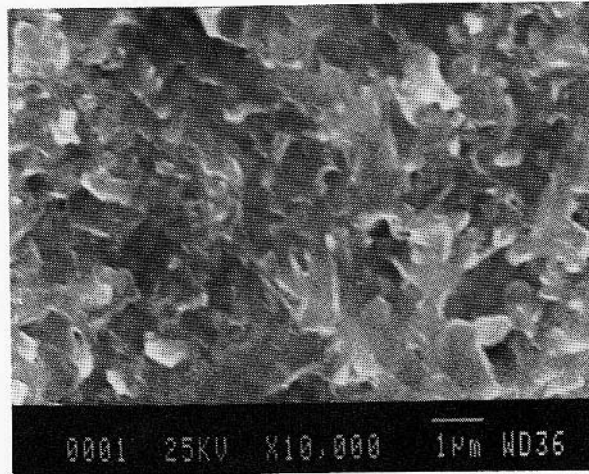


Fig. 2. SEM photograph of a GTE PY6 specimen.

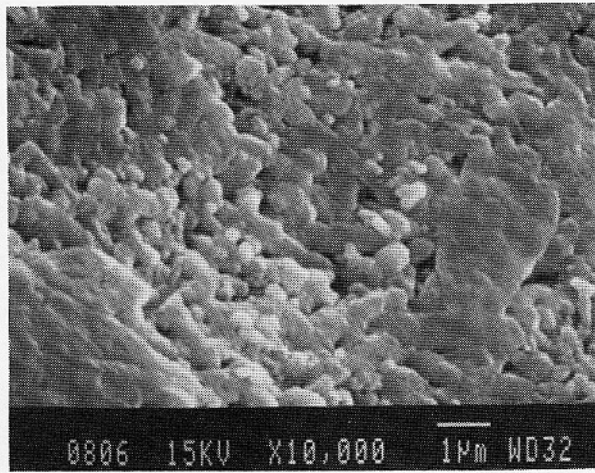


Fig. 3. SEM photograph of a GTE PY6 specimen tested at 1450°C.

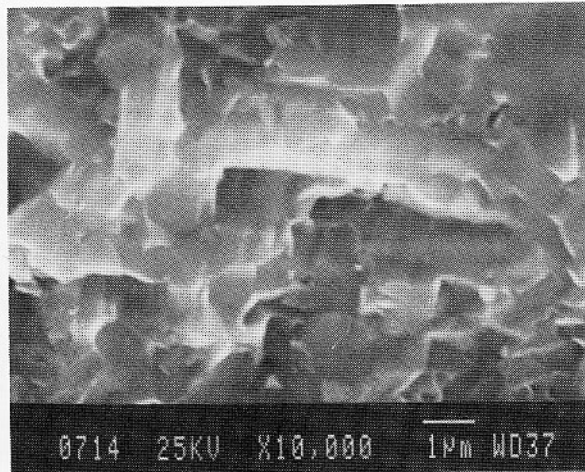


Fig. 4. SEM photograph of a Norton Noralide XL144 specimen.

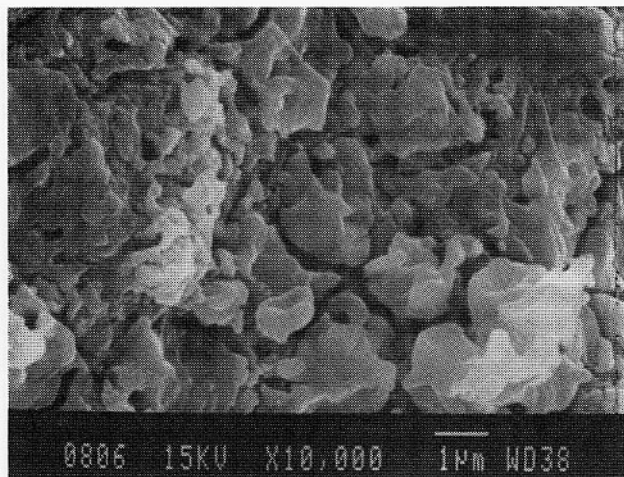


Fig. 5. SEM photograph of a Norton Noralide XL144 specimen tested at 1450°C.

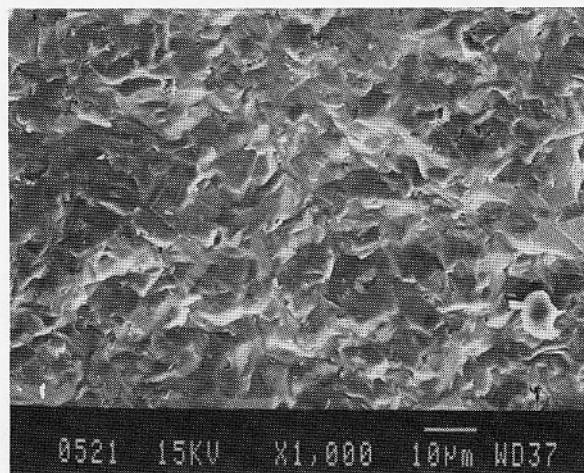


Fig. 6. SEM photomicrograph of a Sohio Hexoloy SA specimen.

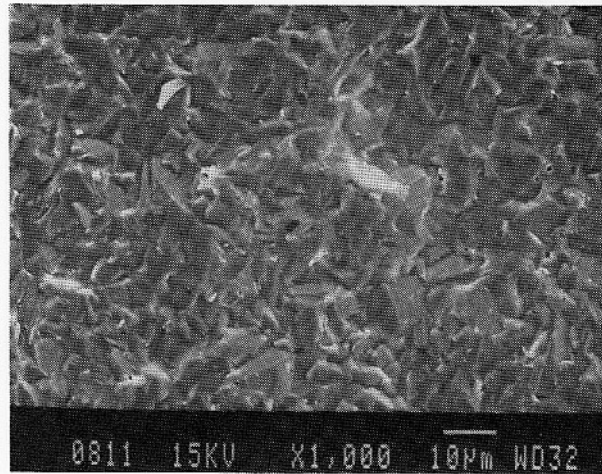


Fig. 7. SEM photomicrograph of a Sohio Hexoloy SA specimen tested at 1450°C.

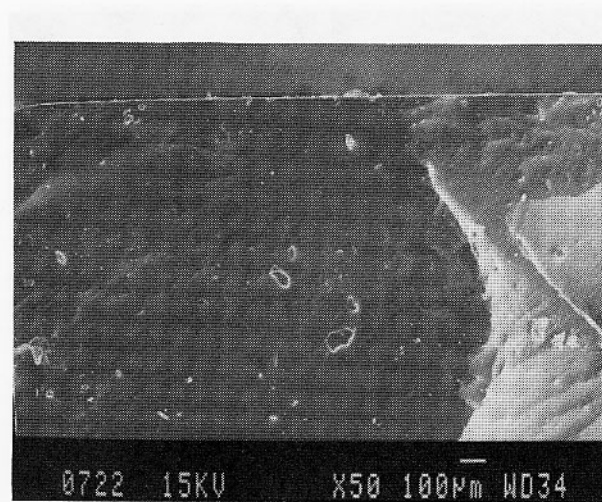


Fig. 8. Fracture surface of PY6 specimen tested at 1450°C (fracture initiated at inclusion).

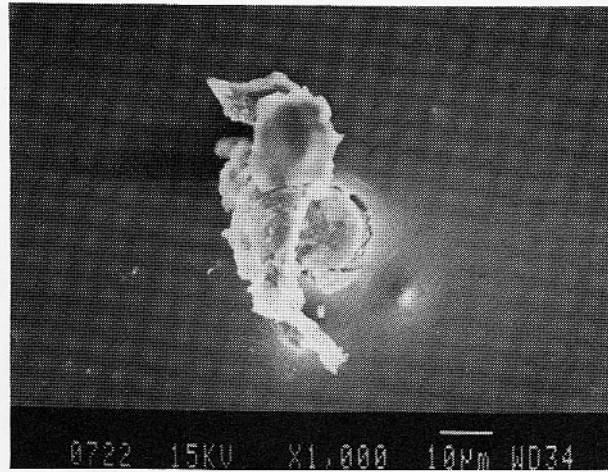


Fig. 9. Inclusion at fracture site, enlarged view.

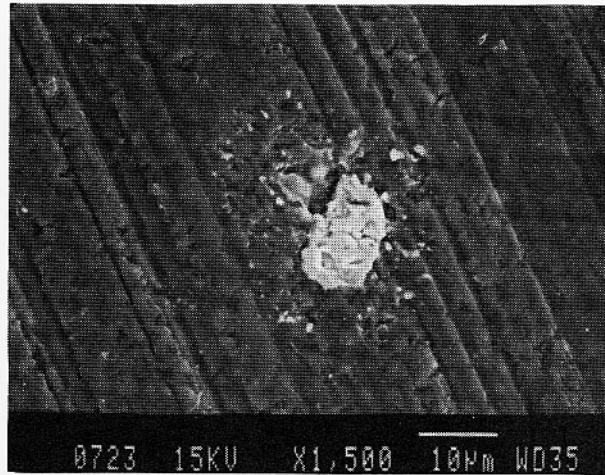


Fig. 10. Inclusion on surface of an untested PY6 specimen.

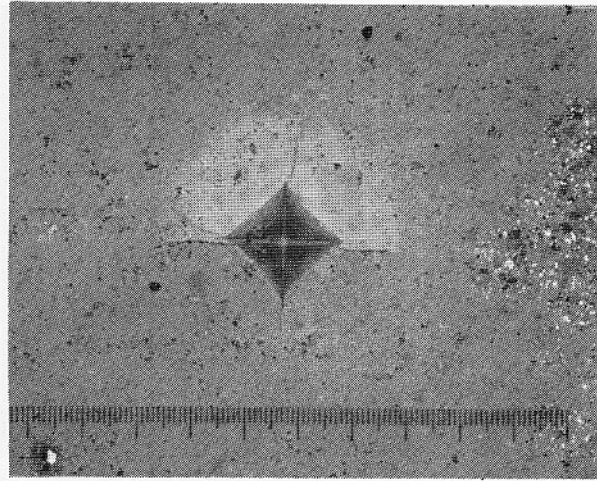


Fig. 11. Typical indent for GTE PY6.

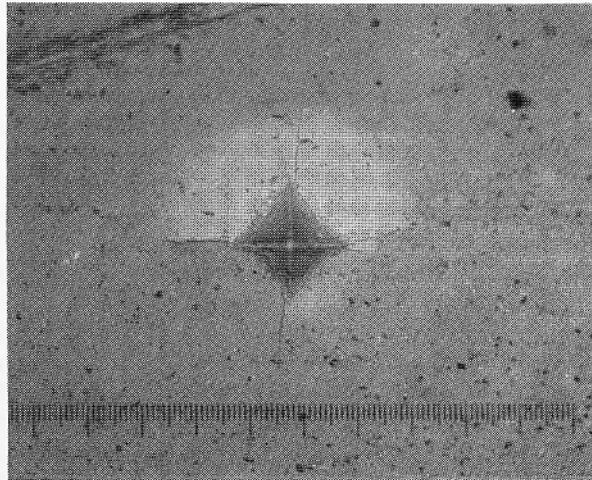


Fig. 12. Typical indent for Noralide XL144.

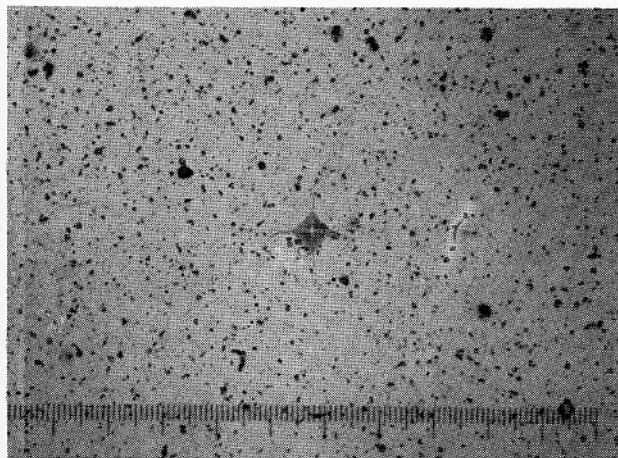


Fig. 13. Typical indent for Hexoloy- α -SiC.

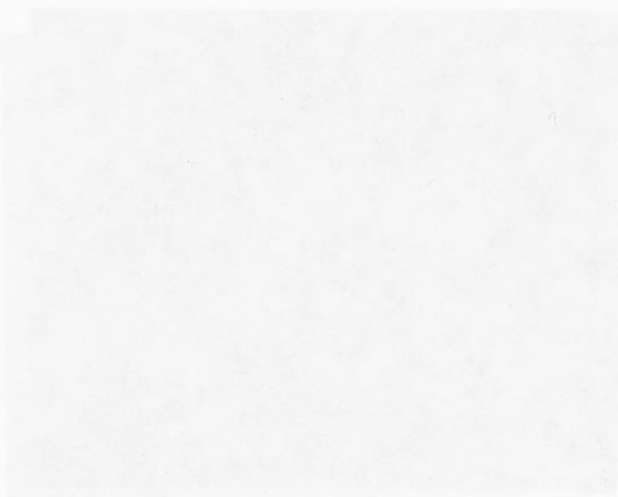


Fig. 14. Typical indent for Pionite (SiO₂).